Growth of South Rough Ridge, Central Otago, New Zealand: Using in situ cosmogenic isotopes and geomorphology to study an active, blind reverse fault

Eleanor R. Bennett,[1] John H. Youngson,[2] James A. Jackson,[1] Richard J. Norris,[2] Grant M. Raisbeck,[3] Françoise Yiou,[3] and Eric Fielding[4]

Received 19 May 2004; revised 7 December 2004; accepted 20 December 2004; published 24 February 2005.

[1] In situ cosmogenic ^{10}Be and ^{26}Al measurements on sedimentary quartzites, together with analysis of abandoned river terraces, can be used to show how drainage responded to the lateral propagation of a late Quaternary anticline forming above a blind reverse fault in Central Otago, New Zealand. A close link between the progression of cosmogenic ages and the tectonic geomorphology allows us to confirm that uplift and propagation rates on the anticline are in the ranges 0.08–0.12 mm yr^{-1} and 0.8–1.5 mm yr^{-1}, respectively, over the last 550,000 years. The agreement between the isotopic and geomorphological evidence in turn requires that minimum ^{10}Be exposure ages as great as 660 ka are not in steady state with respect to erosion. This is a geochemical result of significance, as it opens the possibility of a more regional analysis of landscape evolution in this region, using the same rocks. On an adjacent anticline, thought to be even older on geomorphological arguments, ^{10}Be concentrations give minimum exposure ages in the range 750–1400 ka. These extremely old minimum ages are rare worldwide, as they are usually limited to smaller values by erosion. They are attributable to the very resistant nature of the quartz-rich boulders in which the measurements were made, which in places are shown to have erosion rates lower than 0.5 mm kyr^{-1}.

Citation: Bennett, E. R., J. H. Youngson, J. A. Jackson, R. J. Norris, G. M. Raisbeck, F. Yiou, and E. Fielding (2005), Growth of South Rough Ridge, Central Otago, New Zealand: Using in situ cosmogenic isotopes and geomorphology to study an active, blind reverse fault, *J. Geophys. Res.*, *110*, B02404, doi:10.1029/2004JB003184.

1. Introduction

[2] In actively deforming regions, faults create the landscape by repeatedly slipping in earthquakes. The landscape therefore contains signals which, if read correctly, tell us about fault development and can greatly enhance the information about active tectonics available from other sources, such as earthquake seismology and geodesy. With this in mind, we have investigated the evolution of a young buried reverse fault beneath an anticline in the Central Otago region of the South Island, New Zealand, using both in situ cosmogenic isotopes and geomorphology. This is a region where we had earlier used observations of geomorphology and drainage to make qualitative inferences about the relative ages of faults and their propagation directions [*Jackson et al.*, 1996]. Then, in a preliminary study of in situ cosmogenic ^{10}Be concentrations, we demonstrated that these earlier inferences were, in principle, correct and that the fault growth has been active over the last 500,000 years [*Jackson et al.*, 2002]. However, the ^{10}Be measurements also suggested that evolution of the fault-related geomorphology was not continuous, but episodic, in a manner that we could not explain. Now, with additional cosmogenic isotope measurements, including both ^{10}Be and ^{26}Al, and a more detailed examination of the geomorphology, we can show how the geochemical and landscape observations are connected, which is the principal purpose of this paper. We also investigated petrological influences on the erosional behavior of the rocks sampled, which provide insights that will guide future sampling programs for cosmogenic studies.

2. Geological and Tectonic Setting

[3] In the Central Otago region of the South Island of New Zealand, the development of asymmetric anticlines above buried reverse faults has exposed elongated ridges of basement schist as the overlying Tertiary sediments are uplifted and eroded, which occurs rapidly once uplift begins [*Youngson et al.*, 2005]. The Tertiary sediments were deposited on an erosion surface of probable late Cretaceous to early Miocene age [*Bishop*, 1994] cut into the schist,

[1]University of Cambridge, Department of Earth Sciences, Bullard Laboratories, Cambridge, UK.
[2]Department of Geology, University of Otago, Dunedin, New Zealand.
[3]Centre de Spectrométrie Nucléaire et de Spectrométrie de Masse, Institut National de Physique Nucléaire et de Physique des Particules, CNRS, Orsay, France.
[4]Jet Propulsion Laboratory, Pasadena, California, USA.

0148-0227/05/2004JB003184$09.00

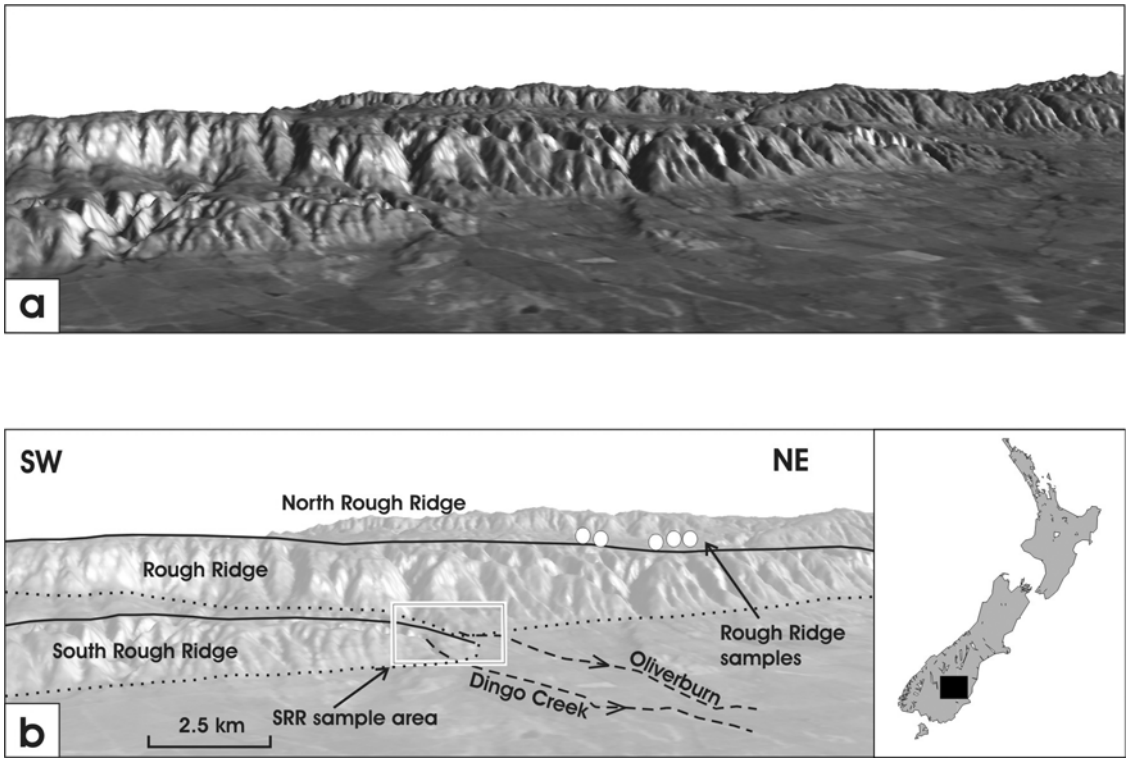

Figure 1. (a) Perspective view looking NW of the Rough Ridge system of ranges in Central Otago. The image was made by draping a Landsat 7 image over a digital elevation model (DEM) from the Department of Survey and Land Information (DOSLI), New Zealand. (b) Annotated version, showing the low South Rough Ridge dying out to the NE in front of the higher parallel Rough Ridge, with the solid black lines being the crest lines of each ridge and the dotted lines being the bases of the steep range flanks. Sample sites for cosmogenic isotope analysis on Rough Ridge are shown by open circles, with the two on the left being close to the ridge crest and the others being farther north (Rough Ridge plateau/flank of North Rough Ridge). The sample area on South Rough Ridge is marked by the box. Inset shows the location of Central Otago (black box) in the South Island of New Zealand.

which provides a useful reference surface for evaluating the late Cenozoic deformation. Near the base of the Tertiary sequence are patchy occurrences of very hard silica-cemented horizons formed originally by diagenesis within the quartz-rich sediments. They occur typically within 1–3 m of the old erosion surface. These horizons now form stone pavements of large boulders and slabs up to 4m thick on the schist after the rest of the Tertiary sediments have been eroded [*Jackson et al.*, 2002; *Cotton*, 1917]. The very resistant lithology of the boulders results in their preservation during erosion of surrounding sediments and underlying schist. The occurrence of these boulders is patchy as they are Miocene fluvial channel sediments [*Youngson et al.*, 1998], mainly quartz-pebble conglomerates and quartz sandstones. In the area of interest here, a Miocene fluvial channel crossed an area of the erosion surface which now forms the crest of South Rough Ridge and adjacent strath terraces. Discrete fields of these quartzite boulders exist elsewhere in Central Otago [*Youngson et al.*, 2005]. The fact that these fields have such well-defined boundaries demonstrates that the boulders have not moved significantly during or after emplacement on the schist surface.

[4] The scattered boulders, known locally as ''sarsen stones,'' are made of almost pure quartz, and are an ideal target for in situ cosmogenic ^{10}Be and ^{26}Al analysis. This study, and that of *Jackson et al.* [2002], focuses on the propagating tip of one of the anticline ridges, called South Rough Ridge (Figure 1).

[5] The situation prior to this current study is summarized in Figure 2. South Rough Ridge is a relatively low anticline, parallel to the higher Rough Ridge (Figures 1 and 2a). Prominent dry valleys (''wind gaps'') along the crest of South Rough Ridge indicate that streams once flowed across it from Rough Ridge. Those streams were diverted by the uplifting frontal ridge and their catchments combined into larger streams that still cross the line of the ridge in the gorges, for example at Dingo Creek in Figure 2b. All the streams crossing South Rough Ridge have asymmetric catchments, with their drainage arising from south of the gorges (Figure 2b). These observations led *Jackson et al.* [1996] to conclude that South Rough Ridge was both younger than Rough Ridge and propagating northward. These conclusions were verified by in situ ^{10}Be measurements along the northern 600 m of the nose of South Rough Ridge near Oliverburn, showing a progression of minimum exposure ages from 550 ka in the south to 100 ka in the north (Figure 2c), and by much older minimum exposure ages of 900–1050 ka on the higher crest of Rough Ridge itself [*Jackson et al.*, 2002]. Although the age progression in Figure 2c is consistent with an average propagation rate of

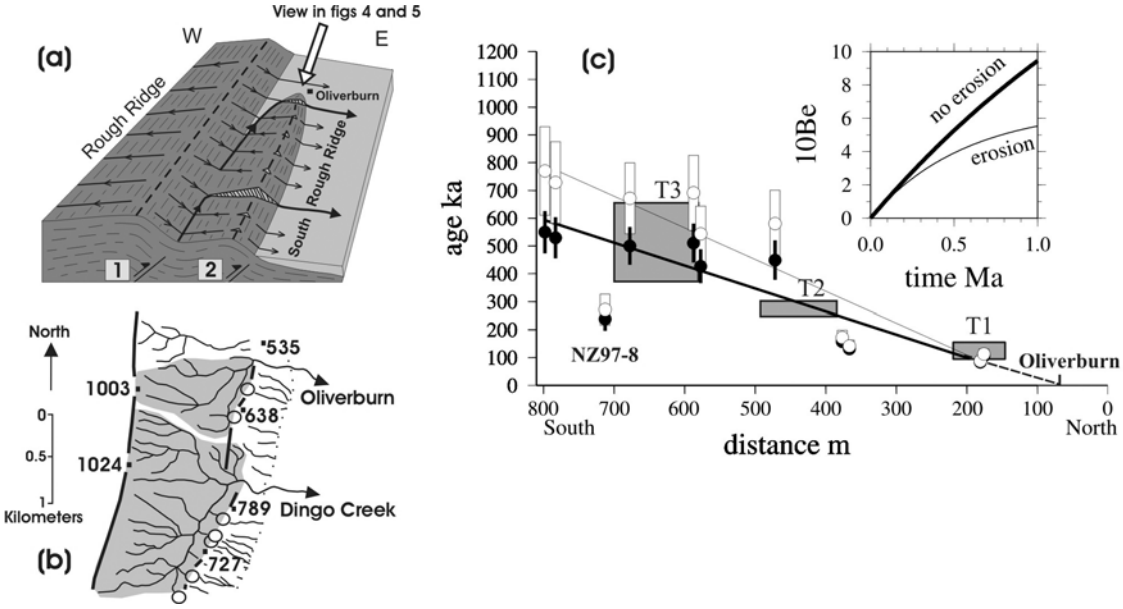

Figure 2. (a) Schematic cartoon illustrating the structure and drainage around the tip of South Rough Ridge. (b) Detail of the drainage system around the tip of South Rough Ridge (adapted from *Jackson et al.* [1996]). Solid black lines are drainage divides on the crests of Rough Ridge (west) and South Rough Ridge (east). Open circles are dry valleys (wind gaps) on the crest of South Rough Ridge; numbers are spot heights in meters. Shaded areas are the drainage catchments of Oliverburn and Dingo Creek. The asymmetry of the river catchments feeding the gorges through South Rough Ridge and the positions of wind gaps along its crest suggest that the blind fault beneath South Rough Ridge (2 in Figure 2a) is younger than that beneath Rough Ridge (1) and is also propagating north [*Jackson et al.*, 1996]. (c) Plot of ^{10}Be ages against distance along the nose of South Rough Ridge (adapted from *Jackson et al.* [2002]). Ages have been recalculated using a sea level, high-latitude production rate of 4.53 atoms g^{-1} (see Table 1 footnotes). Solid circles are minimum ages assuming no erosion, with error bars (the assigned 10% error in production rate dominates the error from the measurement of nuclide concentration) representing extreme possible ranges. Open circles and open error bars are the maximum ages and their equivalent extreme ranges allowing for the maximum erosion rate in the region (see section 5). Straight lines fitted to the data give propagation rates of 1.3 mm yr^{-1} with no erosion (thick line) or 0.8 mm yr^{-1} allowing for erosion (thin line). Shaded boxes mark the positions and ages of the terraces T1–T3 crossing the ridge crest, based on the new data presented in this paper (see text). The inset shows the expected evolution of ^{10}Be concentration (10^6 atoms g^{-1}) with time at the top of Rough Ridge with no erosion (thick line) and allowing for erosion (thin line), with the erosion rate calculated assuming the samples at the top of Rough Ridge have reached saturated steady state values.

0.8–1.5 mm yr^{-1} for the anticline tip over the last 550 kyr, the actual ^{10}Be minimum exposure ages appear to cluster into two groups, of 450–550 ka in the distance range 500–800 m and of 100–170 ka in the range 200–400 m. When examined more closely, new geomorphological evidence (described below) shows that this clustering is real and easily explained. Additional cosmogenic isotope measurements also help to clarify and confirm this analysis. By connecting the geomorphology and cosmogenic measurements in this way, we can demonstrate that the ^{10}Be concentrations in the rocks we sampled are not in steady state with respect to erosion, even though their minimum ages are several hundred ka. This important result confirms the potential of these rocks for wider landscape evolution studies of this region.

3. New Geomorphological Observations

[6] New geomorphological analysis shows that the deflection of the Oliverburn stream round the propagating northern tip of South Rough Ridge was not a continuous process, but occurred as a series of discrete events. The evidence for this conclusion is a series of E-W strath terraces west of the South Rough Ridge axis, cut into the schist by the Oliverburn stream, which were progressively uplifted and abandoned as the stream was deflected north (Figures 3 and 4). With an accurate, newly available, digital elevation model from the NASA Topographic Synthetic Aperture Radar (TOPSAR) mission and new digital air orthophotos from Land Information New Zealand (LINZ), these terraces can now clearly be traced in maps and profiles (Figure 4 inset and Figure 5). The lower terraces T1, T2 and T3 in Figures 3–5 can all be traced across the axis of South Rough Ridge, with T2 and T3 corresponding to the wind gaps identified by *Jackson et al.* [1996] either side of the 638 m spot height in Figure 2b. Elevation profiles along those terraces (Figure 6b) and perpendicular to the ridge are shown in Figure 7a. The height difference between T1, T2, and T3 on the west side of the axis of South Rough Ridge is greater than on the east side due to uplift on South Rough

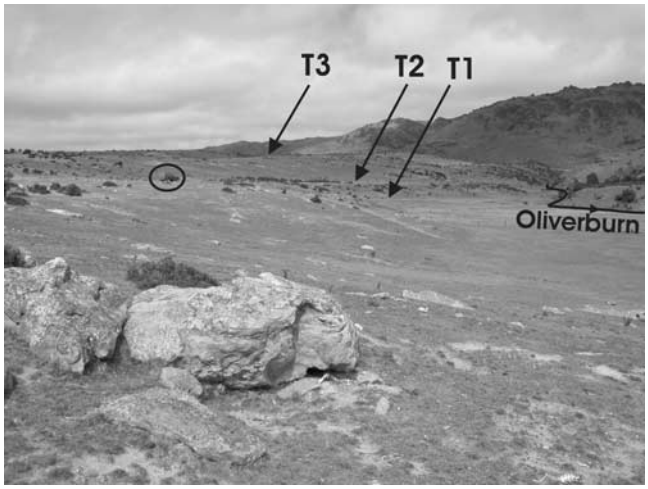

Figure 3. View WSW from the northern tip of South Rough Ridge, showing the three terraces T1–T3 above the Oliverburn stream, also shown in Figures 4–7. In the foreground is a quartzite boulder on terrace T1, where other boulders gave minimum ^{10}Be ages of 103–178 ka. Note the car (circled) on T2, for scale.

Ridge. The lowest terrace (T1) is essentially parallel to the Oliverburn stream itself, but is ~7 m higher (Figure 7b). This terrace is not visibly affected by the topographic expression of the ridge, so the 7 m elevation change is mostly due to a change in regional base level. To the east of the ridge, T2 is ~7 m higher than T1, but to the west of the ridge the elevation change is ~27 m, indicating that this terrace has been uplifted ~20 m after abandonment. The same can be seen for the highest terrace, T3, which to the east of the ridge is ~13 m higher than T1 but on the west side of the ridge crest is on average 40 m higher than T1. Therefore the terraces have been progressively uplifted and warped on the west side of the ridge by the continuing growth of the ridge. Since the terraces continue to the east of the topographic expression of South Rough Ridge, one of the reasons for terrace formation must have been regional base level changes. These erosional terraces are preserved because of the continuing northward deflection of the Oliverburn by the propagating ridge. Incision events are then likely to be due to the interplay between local tectonic uplift, regional base level changes and changing climatic conditions. A 2 m high knickpoint in the Oliverburn just upstream of the axis of South Rough Ridge is not associated with any lithological variation and demonstrates that local tectonic uplift is a component of strath terrace formation. Thus, regardless of whether or not the ridge itself grew continuously, the response of the drainage system to that growth was not continuous, but episodic, with the Oliverburn being deflected north and incising in discrete (or rapid) events as the ridge was uplifted.

[7] It is now clear that in our earlier study [*Jackson et al.*, 2002], by sampling along the ridge axis itself, we sampled the remnants of discrete terrace levels, and hence sarsen stones that were exposed while the Oliverburn occupied those levels, which is why our ^{10}Be dates are clustered in Figure 2c. In order to test this interpretation of the geomorphology, we sampled sarsen stones for cosmogenic isotope analysis from sites on the terraces west of the ridge axis.

4. Sampling and Analytical Procedure

[8] As part of this present study, we revisited all the sites sampled and measured earlier, to reflect on our sampling strategy in the light of our ^{10}Be analyses. We always sampled from the tops of large slabs (typically 4–10 m^2 or bigger) that appeared to be in situ, firmly embedded in the soil, and showed no signs of recent dislodgement. We avoided slabs on steep slopes, where they might have slid or rolled to new positions. Bedding can be identified in the boulders, and we only sampled from boulders which were the right way up. Some toppling of the boulders may occur as the 1–3 m of underlying sediment is eroded, but as sediment stripping occurs rapidly, this is only a problem early on in the exposure history of the boulder, and is unlikely to significantly affect our results. Generally, all our previous sites stood at least several tens of cm above the soil. However, one of them (NZ97-8), which had an

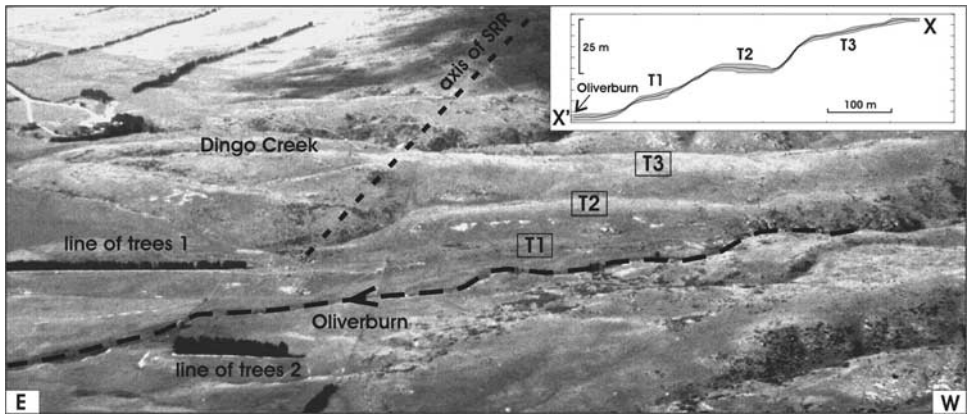

Figure 4. Oblique air photo looking south from the northern tip of South Rough Ridge (see Figure 2a), showing terraces T1–T3 and the lines of trees marked in Figure 5. Inset shows a cross section, taken from the topographic synthetic aperture radar (TOPSAR) DEM, along line X-X′ in Figure 6b, parallel to the axis of South Rough Ridge and across terraces T1–T3 on the west side of the ridge. The shaded width of the profile shows the height variations within a swath 50 m wide along the section.

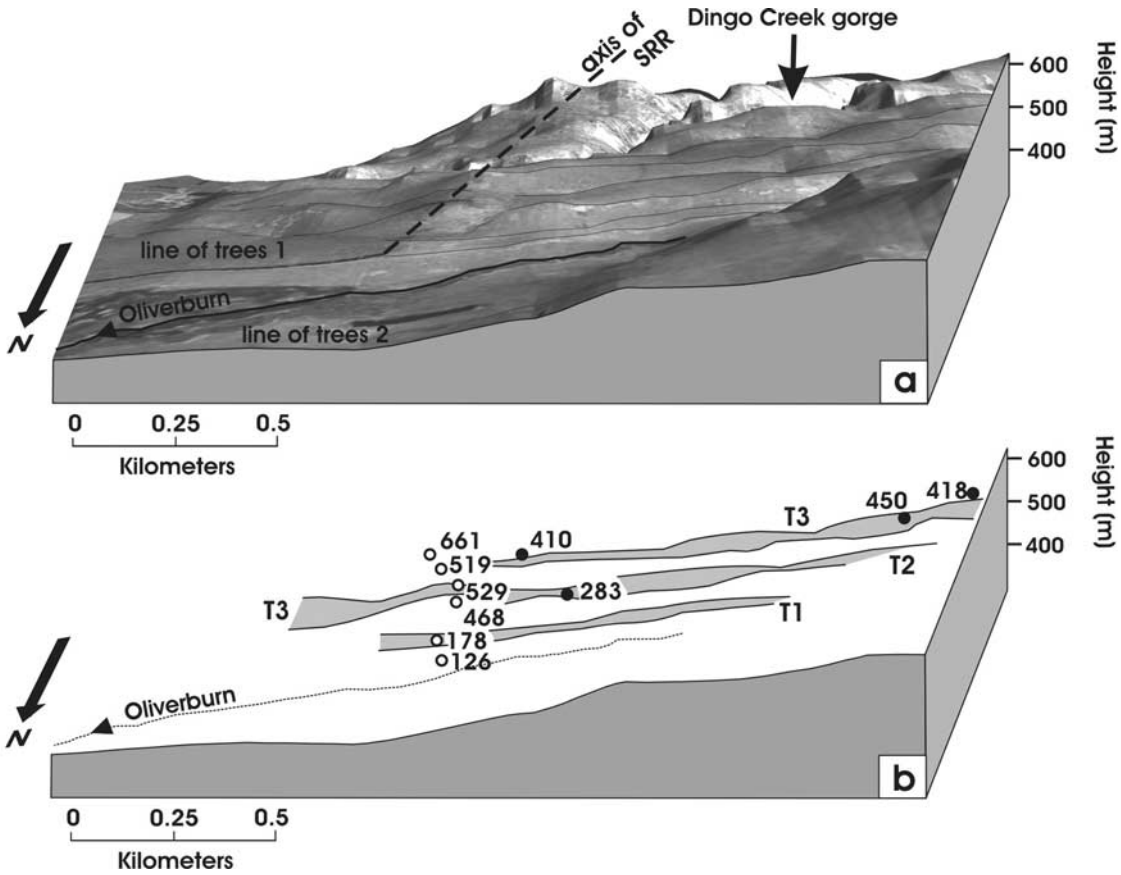

Figure 5. Perspective views looking south at the tip of South Rough Ridge (see Figure 2a). This view was constructed from the NASA TOPSAR DEM, overlain by an air orthophoto from LINZ. (a) Flat surfaces of terraces T1–T3, marked by thin parallel lines. The lines of trees marked 1 and 2 mark the positions of trees visible in Figure 4. (b) Flat surface of terraces T1–T3, shaded. Note that T3 is warped around the crest of the ridge and therefore appears lower down on the eastern side of the crest than on the western side. The oblique view makes T3 look much narrower than it is (see Figure 6). Open circles are sample sites on the crest of South Rough Ridge; solid circles are sample sites on terraces T2 and T3. At each site, two boulders were sampled. The adjacent numbers are the oldest apparent ^{10}Be ages from each pair at each site, in ka. (For all the ages, see Figure 6.)

anomalously young minimum ^{10}Be age for its position (see Figure 2c), was virtually at soil level and clearly at greater risk from partial burial during its history than the others. With our new experience, we would not have sampled this site.

[9] The sarsen stones can be quite varied in character. Some are massive quartz-pebble conglomerates or breccias, cemented by quartz. Others are relatively fine grained, homogeneous sands, also with quartz cements. All those we sampled were essentially pure quartz with pure quartz cement, were extremely hard, and very difficult to break. We generally took samples from two boulders or slabs at each site. We avoided any that looked impure, or showed signs of exfoliation or bedding-parallel splitting during weathering, except for one (discussed later) that we deliberately sampled to show that such effects lead, as expected, to higher erosion rates.

[10] The samples were crushed and sieved to yield 0.25–1.0 mm fragments, which were then cleaned in HCl and sequentially leached in HF to eliminate potential surface contamination by ^{10}Be produced in the atmosphere [*Brown et al.*, 1991]. The pure quartz separates (~30 g) were then dissolved in HF in the presence of ^{9}Be carrier (~250μg). Extraction and separation of beryllium and aluminum was achieved using ion exchange columns, based on the method of *Licciardi* [2000]. The Al and Be hydroxides are then precipitated and heated in quartz crucibles to convert them to oxides. The ^{10}Be/^{9}Be ratio of the resulting BeO was measured relative to National Institute of Technology and Standards (NIST) standard reference material (SRM) 4325 (2.68×10^{-11}) at the Tandétron AMS facility at Gif-sur-Yvette, France [*Raisbeck et al.*, 1987, 1994]. Blanks prepared in parallel with the new samples gave ^{10}Be/^{9}Be ratios in the range of 1 to 6×10^{-14}, with one as high as 1.2×10^{-13}. These values are about 5 times higher than the blanks reported by *Jackson et al.* [2002], for reasons that are not clear, but are still <5% of the smallest measured ratio in the newly sampled quartzites.

[11] After dissolving the quartz in HF and converting to chloride (prior to the ion exchange column chemistry), a small aliquot of the sample was taken to measure the total aluminum content by a Varian Vista inductively coupled

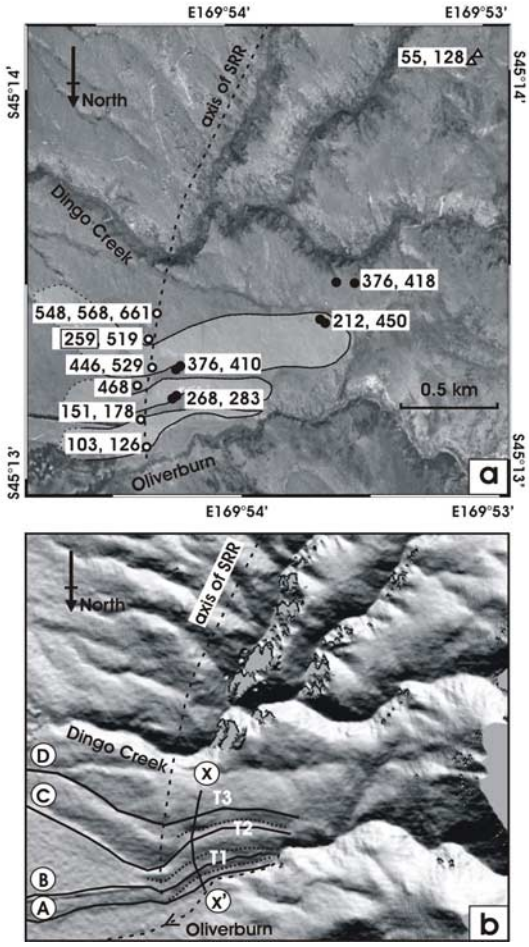

Figure 6. (a) Orthophoto from LINZ showing the locations of sample sites on the crest of South Rough Ridge (open circles), on terraces T1–T3 (solid circles), and at the exfoliating sandstone discussed in section 7 (open triangles). At each site the minimum ^{10}Be ages in ka are shown for both samples (only the oldest is shown in Figure 5). The sample at 259 ka (outlined with a black box) is the anomalous NZ97-8 (see Figure 2c), discussed in the text. Flat terrace surfaces are shaded to indicate the position of the samples with respect to the terraces (see Figure 6b for terrace labels). The dotted lines indicate that tracing the exact terrace extents to the eastern side of the ridge crest is interpretative, as the height difference between the terraces decreases. (b) TOPSAR DEM, illuminated from the south, of approximately the same area as Figure 6a and at approximately the same scale (the look angle is different in each case). X-X′ is the line of the cross section shown in the inset to Figure 4. Solid lines are the lines of the cross sections in Figure 7 along the Oliverburn stream floodplain (A), and terrace surfaces T1–T3 (B–D). Dotted lines are the bases of the terrace risers. The dashed line is the axis of South Rough Ridge.

plasma-atomic emission spectrometry (ICP-AES). The measurements were calibrated with respect to external standards, as this was found to give more reproducible results than calibration by standard additions. The machine calibration was checked against three U.S. Geological Survey rocks with certified concentrations of aluminum. The ^{26}Al/^{27}Al ratio was measured relative to an in-house standard having a ^{26}Al/^{27}Al ratio of 9.8×10^{-11} at Gif-sur-Yvette. Blanks prepared in parallel gave ^{26}Al/^{27}Al ratios of $<1 \times 10^{-14}$, which is less than 0.7% of the lowest measured ratio.

5. Results for ^{10}Be

[12] All our isotopic measurements are presented in Table 1. To interpret these, we first estimated the in situ ^{10}Be production rates (P_0), which are a function of latitude and altitude. We used a high-latitude, sea level production rate of 5.17 atoms g^{-1} yr^{-1} [*Stone*, 2000]. This value was adjusted to allow for the fact that a different accelerator mass spectrometry (AMS) standard was used here compared to that used for most production rate determinations (see caption Table 1). Site-specific production rates are then

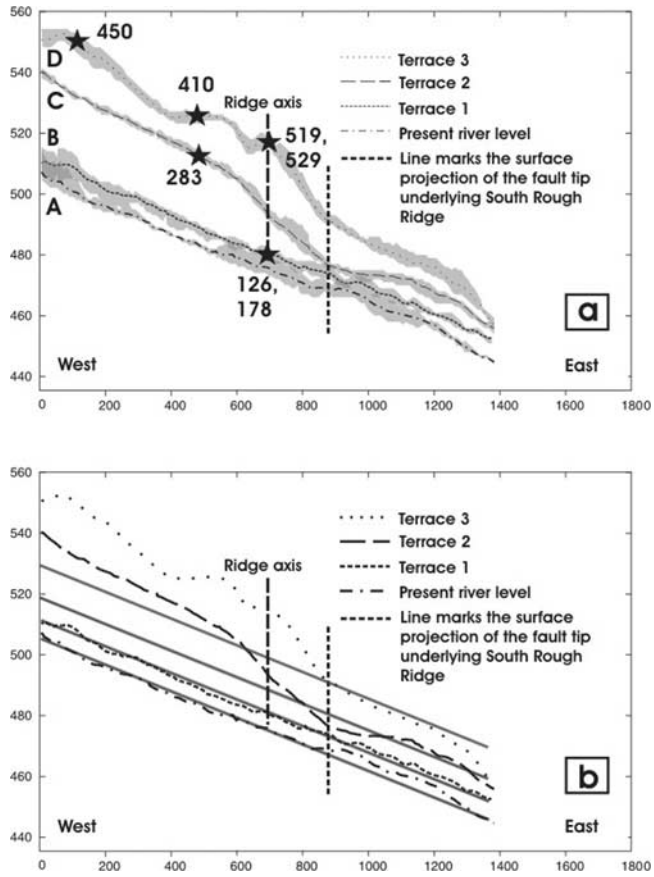

Figure 7. (a) Swath profiles following the flat surfaces of terraces T1–T3 (B–D) and the Oliverburn floodplain (A) across the crest of South Rough Ridge (see Figure 6b for locations). Shaded bounds are extreme height variations along the swaths. Sample locations are extrapolated schematically onto the profiles, and the oldest ^{10}Be age in ka for each pair is given (as in Figure 5b). (b) Plot with variations omitted and with average slopes shown through the terrace surfaces east of the ridge axis. When projected west of the axis, the terraces show the progressively increasing height offset through the sequence T1–T3 (see text).

Table 1. The ^{10}Be and ^{26}Al Concentrations and Calculated Minimum Exposure Ages for the South Rough Ridge and Rough Ridge Samples[a]

Samples	Latitude 45°	Longitude 169°	Height, m	^{10}Be P_0, atoms g^{-1} yr^{-1}	^{10}Be Concentration, 10^6 atoms g^{-1}	Quartz Weight, g	^{26}Al/^{27}Al Ratio 10^{-13}	Total ^{27}Al, mg	^{26}Al Concentration, 10^6 atoms g^{-1}	^{10}Be Age, ka	^{26}Al Age	^{26}Al/^{10}Be
SRR Quartzites												
NZ97-1[b]	13.360	54.525	540	7.25	3.57 ± 0.20					568 ± 76		
NZ97-3[b]	13.360	54.252	540	7.25	3.46 ± 0.20	38.4165	53.6 ± 3.0	5.87 ± 0.29	18.3 ± 1.36	548 ± 74	456 ± 57	5.3 ± 0.5
NZ97-5	13.398	54.320	540	7.25	4.06 ± 0.28					661 ± 96		
NZ97-8[b]	13.330	54.355	530	7.19	1.74 ± 0.21					259 ± 43		
NZ97-6[b]	13.330	54.355	530	7.19	3.27 ± 0.18	13.3786	41.7 ± 4.1	1.83 ± 0.09	12.7 ± 1.41	519 ± 68	297 ± 45	3.9 ± 0.5
NZ97-10[b]	13.277	54.343	520	7.13	3.30 ± 0.19	18.7129	61.9 ± 4.3	2.84 ± 0.14	21.0 ± 1.80	529 ± 70	556 ± 73	6.3 ± 0.7
NZ97-9[b]	13.277	54.343	520	7.13	2.84 ± 0.20					446 ± 61		
NZ97-12[b]	13.213	54.406	510	7.07	2.94 ± 0.26					468 ± 71		
NZ97-16[b]	13.126	54.395	500	7.01	1.19 ± 0.08	30.7152	30.5 ± 2.6	2.36 ± 0.12	5.23 ± 0.51	178 ± 23	115 ± 16	4.4 ± 0.5
NZ97-17[b]	13.126	54.395	500	7.01	1.02 ± 0.07					151 ± 19		
NZ97-18[b]	13.056	54.378	490	6.95	0.70 ± 0.07					103 ± 15		
NZ97-19[b]	13.056	54.378	490	6.95	0.85 ± 0.06	36.3652	21.1 ± 1.8	3.57 ± 0.18	4.62 ± 0.45	126 ± 16	102 ± 14	5.4 ± 0.7
NZ02-50SRR	13.214	54.234	530	6.91	1.82 ± 0.12	31.0884	93.2 ± 3.7	2.20 ± 0.09	14.8 ± 0.83	283 ± 37	373 ± 43	8.1 ± 0.7
NZ02-51SRR	13.200	54.271	530	7.00	1.75 ± 0.11	17.6829	38.4 ± 3.0	1.33 ± 0.05	6.43 ± 0.56	268 ± 34	144 ± 19	3.8 ± 0.4
NZ02-52SRR	13.279	54.230	540	6.96	2.57 ± 0.17	22.2625	48.2 ± 2.4	3.14 ± 0.13	15.2 ± 0.96	410 ± 55	381 ± 45	5.9 ± 0.5
NZ02-53SRR	13.288	54.220	540	6.93	2.37 ± 0.16	37.4190	90.6 ± 3.5	3.76 ± 0.15	20.3 ± 1.13	376 ± 50	552 ± 63	8.6 ± 0.7
NZ02-54SRR	13.366	53.687	600	7.47	3.00 ± 0.20	32.4117	77.3 ± 3.4	3.39 ± 0.14	18.1 ± 1.07	450 ± 61	433 ± 50	6.0 ± 0.5
NZ02-55SRR	13.353	53.667	600	7.31	1.47 ± 0.09	26.2325	47.3 ± 2.4	3.16 ± 0.13	12.7 ± 0.82	212 ± 27	292 ± 35	8.7 ± 0.8
NZ02-56SRR	13.456	53.617	622	7.61	2.86 ± 0.19	42.2615	202.2 ± 5.6	1.65 ± 0.07	17.6 ± 0.86	418 ± 56	409 ± 46	6.2 ± 0.5
NZ02-57SRR	13.455	53.543	630	7.69	2.63 ± 0.17	24.7812	72.0 ± 3.4	2.98 ± 0.12	19.3 ± 1.20	376 ± 50	452 ± 53	7.4 ± 0.7
NZ02-60SRR	14.013	53.062	640	7.49	0.41 ± 0.03	24.2863	13.9 ± 1.4	2.32 ± 0.09	2.97 ± 0.32	55 ± 7	60 ± 9	7.2 ± 0.9
NZ02-61SRR	14.029	53.041	640	7.55	0.94 ± 0.06	36.1302	36.2 ± 2.1	4.20 ± 0.17	9.39 ± 0.66	128 ± 16	200 ± 25	10.0 ± 1.0
SRR Schists												
NZ97-4	13.473	54.459	540	7.25	0.64 ± 0.05					91 ± 12		
NZ97-21[b]	13.676	54.459	550	7.32	0.45 ± 0.03					62 ± 8		
NZ97-22[b]	13.973	54.459	600	7.64	0.60 ± 0.04					80 ± 10		
NZ97-23[b]	14.149	54.351	615	7.73	0.41 ± 0.03					54 ± 7		
RR Quartzites, Ridge Crest												
NZ97-30[b]	11.081	51.757	880	9.64	7.64 ± 0.39					1020 ± 151		
NZ97-32[b]	11.081	51.757	880	9.64	7.86 ± 0.41					1059 ± 159		
NZ97-33	11.081	51.757	880	9.64	6.94 ± 0.45	16.0898	27.4 ± 2.6	10.70 ± 0.54	40.7 ± 4.33	900 ± 137	938 ± 132	5.8 ± 0.6
RR Quartzites, Plateau/Flank of NRR												
NZ02-142RR	10.966	52.524	880	9.26	6.45 ± 0.40	28.5265	428.2 ± 18.3	0.76 ± 0.03	25.6 ± 1.50	864 ± 128	512 ± 59	4.0 ± 0.4
NZ02-143RR	10.429	51.935	870	8.90	5.85 ± 0.36	29.9211	146.3 ± 5.7	2.36 ± 0.09	25.8 ± 1.43	803 ± 117	544 ± 62	4.4 ± 0.4
NZ02-144RR	10.426	51.954	870	9.22	5.91 ± 0.37	36.1761	200.6 ± 6.3	1.43 ± 0.06	17.7 ± 0.90	779 ± 113	327 ± 37	3.0 ± 0.3
NZ02-145RR	09.898	51.858	840	8.92	5.94 ± 0.37	32.9188	115.0 ± 5.6	2.95 ± 0.12	23.0 ± 1.44	816 ± 120	468 ± 55	3.9 ± 0.4
NZ02-147RR	09.722	51.298	820	8.70	8.58 ± 0.53	24.2019	162.9 ± 7.2	1.70 ± 0.07	25.6 ± 1.52	1379 ± 237	556 ± 64	3.0 ± 0.3
NZ02-148RR	09.708	51.288	820	8.78	8.19 ± 0.50	35.3625	245.7 ± 7.1	1.35 ± 0.05	20.9 ± 1.03	1273 ± 212	424 ± 47	2.6 ± 0.2
RR Schist												
NZ97-34	11.081	51.757	880	9.64	0.65 ± 0.06					68 ± 9		

[a]All ^{10}Be samples are measured relative to the certified value for NIST SRM 4325 = 2.68×10^{-11}, and the half-life of 1.34 Myr (listed on the NIST SRM certificate) is used when calculating ages and erosion rates. The sea level, high-latitude production rate of 5.17 atoms g^{-1} [*Stone*, 2000] was determined relative to a value for the NIST SRM 4325 of 3.06×10^{-11}. We therefore adjust this production rate to 4.53 atoms g^{-1}. We assume a sea level, high-latitude production rate for ^{26}Al of 31.02, which is 6 times the ^{10}Be production rate given by *Stone* [2000]. Note that the production ratio ^{26}Al/^{10}Be for our samples is therefore 6.84. Uncertainties for ^{10}Be and ^{26}Al concentration are fully propagated from AMS counting statistics, replication errors, weight of carrier in the case of ^{10}Be and stable Al measurement in the case of ^{26}Al. In order to allow a full assessment of the errors involved for ^{26}Al measurements, ^{27}Al measurements and errors, quartz weight and ^{26}Al/^{27}Al ratios are included. Minimum Be and Al ages are calculated assuming no erosion. Age errors are propagated in quadrature from errors in nuclide concentrations and production rate uncertainty. The 10% production rate uncertainty is not significant when comparing samples over a small geographic region.

[b]Samples are the same as those discussed by *Jackson et al.* [2002], but the ages have been recalculated using a sea level, high-latitude production rate of 4.53 atoms g^{-1}.

calculated using a scaling factor for the site location using the expressions of *Lal* [1991]. Production rates for the NZ02 series of samples were also scaled for the thickness of sample collected [*Gosse and Phillips*, 2001], as the very hard nature of the rock meant that it was sometimes impossible to collect only surface chips. We then calculated minimum exposure ages assuming no initial (inherited) ^{10}Be, using equation (4b) of *Brown et al.* [1991]. To estimate errors in the absolute ages, we assumed an uncertainty in P_0 of 10%, which dominates the assigned errors. There is continuing debate about the appropriate production rate and scaling factors [*Bierman et al.*, 2002; *Bierman and Caffee*, 2002] and the value of NIST standard 4325 [*Hotchkis et al.*, 2000], but for our purposes it is the relative production rates, ^{10}Be concentrations and model ages that are most important, and they are almost independent of the above parameters. In order to compare all the sample sites together, our 16 earlier measurements (NZ97 series) are

included with the 20 new (mostly NZ02 series), reanalyzed with the same production rates and scaling factors. We now have 20 sarsen stone measurements from 10 sites on South Rough Ridge, 9 sarsen stone measurements from 6 sites on Rough Ridge, 5 measurements from schists (4 on South Rough Ridge and 1 on Rough Ridge), and 2 measurements from an exfoliating quartz sandstone.

[13] With no erosion, ^{10}Be concentrations at this latitude and altitude should increase with time until they reach a steady state at which the rates of production and decay are equal at about 18.6×10^6 atoms g^{-1} for the samples on the crest of Rough Ridge, and 13.4×10^6 atoms g^{-1} for the samples on South Rough Ridge, which is much more than anything measured in our samples. The effect of erosion is to remove ^{10}Be, causing the steady state to be achieved sooner and at lower concentrations (Figure 2c, inset). A single ^{10}Be concentration is therefore fundamentally ambiguous, yielding either a minimum exposure age or a maximum erosion rate for that latitude and elevation. All the ^{10}Be ages from sarsen stones on the top of Rough Ridge are older than the oldest measured on South Rough Ridge itself (Table 1), with minimum ages for the Rough Ridge crest of 900–1059 ka, and as old as 1379 ka on the Rough Ridge plateau/flank of North Rough Ridge, compared with a maximum of 661 ka for South Rough Ridge. The Rough Ridge samples prove that the sarsen stones are capable of reaching ages well beyond those of South Rough Ridge before reaching steady state. From geomorphological arguments, the exposure of Rough Ridge is expected to predate that of South Rough Ridge (Figures 2a and 2b), so *Jackson et al.* [2002] used these isotopic observations to conclude that the South Rough Ridge samples were probably not in steady state with respect to erosion. If we then assume that the sarsen stones on the Rough Ridge plateau have reached steady state, we can estimate the maximum possible erosion rate that would allow saturation to occur at those concentrations (see *Brown et al.* [1991, equation 3], using an attenuation path length of 150 g cm^{-2}), which is 1.18×10^{-4} g cm^{-2} yr^{-1} or 0.4×10^{-3} mm yr^{-1} if we assume an average density of 2.7 g cm^{-3}. These maximum erosion rates can be used to estimate the maximum possible corrections that can be made to the minimum ages on South Rough Ridge. These corrections increase the ages by ~50% at 500 ka and by ~5% at 100 ka. Such age corrections and erosion rates are maximum values: there is no guarantee that the sarsen stones on the top of Rough Ridge are really in steady state, and their concentrations are still much less than the erosion-free saturation level of 18.6×10^6 atoms g^{-1}.

[14] All the South Rough Ridge sarsen stone sites are shown in Figure 6a. At most sites, the two samples from separate boulders give roughly similar minimum ages, but there are two substantial exceptions. One anomaly is NZ97-8 on the ridge crest (259 ka), which we have already discussed above (Figure 2c), and discard. The other is the pair NZ02-54 (450 ka) and NZ02-55 (212 ka). Most effects we can envisage, such as partial burial during exposure history or enhanced erosion, will tend to reduce the apparent age. Only inherited ^{10}Be from earlier exposure can increase the apparent age, and for reasons discussed by *Jackson et al.* [2002] this is unlikely to be a problem here. Therefore the oldest of a pair of ages is likely to be closer to the true exposure age, and we have simplified the presentation of these results by showing only the oldest apparent minimum age in each site pair on the perspective view in Figure 5b; but all the ages are shown in Figure 6a. Figure 5b shows the age progression along the South Rough Ridge axis (open circles) and also the greater age of the terrace T3 (410–529 ka) compared with T2 (283 ka) and T1 (178 ka). Note that the higher terraces do not project directly (i.e., perpendicular) on to the ridge axis, but are deflected by the axis as they cross it (Figures 5 and 6). Terrace T2 crosses the ridge axis between the sample sites at 178 and 468 ka, while T3 crosses the axis between the 468 and 519 ka sites.

[15] The ^{10}Be measurements therefore support the interpretation of the geomorphology outlined in section 3, with a set of progressively higher and older terraces from the ancestral Oliverburn deflected and uplifted by the propagating axis of South Rough Ridge. The alternative is to argue that all ^{10}Be concentrations are saturated with respect to erosion, which would require erosion rates to vary systematically and inversely with altitude (those at lowest elevation being the fastest), and also spatially in such a way as to precisely, and misleadingly, correlate with the terrace morphology: which seems extremely far-fetched and unlikely. The simplest interpretation, consistent with both the geomorphology and relative minimum ages, therefore requires the ^{10}Be concentrations on South Rough Ridge to have not yet reached steady state with respect to erosion, even though they are as old as 661 ka (minimum) or 1004 ka (maximum, assuming the samples on Rough Ridge are saturated, with an erosion rate of 0.4×10^{-3} mm yr^{-1}).

[16] Meanwhile, all the schist samples (4 on South Rough Ridge, south of Dingo Creek, and 1 on Rough Ridge near site NZ97-33) are almost certainly saturated, with much lower minimum ages of 54–91 ka, whereas their expected ages are >661 ka on South Rough Ridge and ≥900 ka on the crest of Rough Ridge. These minimum ages correspond to erosion rates of the order of 10^{-2} mm yr^{-1} in the schist, or roughly 20 times faster than the maximum erosion rates in the sarsen stones, which is no surprise. This differential erosion rate is corroborated by field evidence. In a few places we see quartzite boulders resting on schist pedestals, as the boulder protects the patch of underlying schist from erosion, while the surrounding schist is subjected to a faster erosion rate. These boulders can topple off their pedestal, and in this case we see bedding at an obvious angle to the schist surface, or that the boulder has broken into pieces.

[17] The sarsen stones on Rough Ridge are interesting in their own right. Their minimum ^{10}Be ages of up to 1379 ka are among the oldest found anywhere, comparable to those reported in parts of Antarctica [*Brook et al.*, 1995] and Australia [*Bierman and Caffee*, 2002], corresponding to extraordinarily low maximum erosion rates of order 0.3 mm kyr^{-1}. Given that the ~660 ka ages on South Rough Ridge are not saturated, there must be a possibility that, even at minimum ages of ~1000 ka on the crest of Rough Ridge, the sarsen stones may not be in steady state with respect to erosion.

6. Results for ^{26}Al

[18] We measured ^{26}Al concentrations in 16 of the new (NZ02 series) and 6 of the old (NZ97 series) sarsen stone samples, with a view to trying to resolve the ambiguity

Figure 8. (a) Photo of exfoliating sarsen stone at sample sites 60 and 61 (note compass for scale). The top layers are being lost quickly because of exfoliation along bedding planes and the clay-rich nature of the rock. (b) Photo of sarsen stone at sample site NZ02-57. This is a typical example of all of the other sarsen stones sampled, which were not eroding in such an obvious manner when compared with those at samples sites 60 and 61.

between exposure age and erosion. The ^{27}Al and ^{26}Al measurements, the ^{26}Al/^{10}Be ratios, and the resulting minimum ^{26}Al ages are shown in Table 1.

[19] For many of the sample sites on South Rough Ridge the minimum ^{26}Al ages are similar to, and roughly track, the minimum ^{10}Be ages, but there are several anomalies (e.g., NZ97-6 and NZ02-51,53,55). The age anomalies are far worse for the older samples on Rough Ridge. There is a great deal of scatter in the ^{26}Al/^{10}Be ratios, and it seems likely that these problematic ratios are the result of some undetected analytical problem, such as the measurement of ^{27}Al. We find that others have had similar problems [*Vance et al.*, 2003].

[20] The measurement of ^{26}Al concentration along with ^{10}Be in a sample should make it possible to place further constraints on the sample's exposure and erosion history. As in most other similar studies we have seen (e.g., four case studies outlined by *Bierman et al.* [2002] and *Belton et al.* [2004]), the formal errors for ^{26}Al concentrations are greater than for ^{10}Be, and dominate the values of the ^{26}Al/^{10}Be ratios. Unfortunately, even for the samples with the smallest of errors, the magnitude of the error makes it impossible to distinguish between exposure age and erosion rates (a conclusion also reached by others, such as *Bierman and Caffee* [2002]).

7. Lithological Influences on Erosion Rates

[21] Finally, in order to improve our understanding of the preservation and erosion controls in the sarsen stones, we analyzed two samples (NZ02-60, 61) from a site between South Rough Ridge and Rough Ridge, marked by triangles in Figure 6a. At this place, the quartzites occur as bedded slabs of fine grained sandstone, cemented but relatively porous, and clearly exfoliating parallel to original bedding (Figure 8). With such an appearance in outcrop, we would not ordinarily have sampled this site, but we did so in the expectation that it would show a relatively young minimum age or high maximum erosion rate, even though its location would suggest a real age substantially older than the oldest age of 661 ka found at the nose of South Rough Ridge. This expectation was confirmed, with minimum ^{10}Be ages for the two samples of only 55 and 128 ka. For the difference in nuclide concentration (and hence calculated exposure age) to be due to erosion, around 50cm of material must have been eroded relatively recently. The low exposure ages may be because the bulk of the rock is simply more friable and more easily eroded everywhere, as it was certainly less well cemented and easier to break than the quartzites we sampled in earnest, and the lower age is similar to those found in the schists. An alternative explanation is that the style of erosion is by exfoliation of bedding-parallel slabs, abruptly removing layers of material and suddenly exposing new bedding surfaces beneath (Figure 8). The surface relief on these boulders is on the order of 30 cm, and there are numerous exfoliated sheets scattered on the ground beside the boulders. The older age (128 ka) was from a prominent remnant knob, while the younger age (55 ka) at the same site was from the top of a flat, lower, bedding surface, which we interpret to have been exposed by exfoliation relatively recently. The reason for the contrast between this site and others is apparent when thin sections of NZ02-61 (minimum ^{10}Be age 128 ka) and NZ02-52 (410 ka) are compared (Figure 9). Both consist of at least 95% quartz grains, but in NZ02-52 the grains are interlocked with undulating sutures and all pore space is filled with cement, whereas in NZ02-61 the grains are not sutured, the interstices are partially open, and the matrix contains some clay minerals, which probably swell when wet and contribute to the mechanical weakening of the rock. NZ02-52 was a typical "hard" quartzite of the sort we sampled elsewhere in this study: massive, very difficult to break, with no sign of erosion by slab exfoliation.

[22] This result is important, demonstrating the necessity of petrographical analysis before lengthy sample processing is begun. In order to compare exposure ages, the samples must be petrologically similar, otherwise lithologically controlled erosion rates may dominate the patterns. We took thin sections of many of our samples to

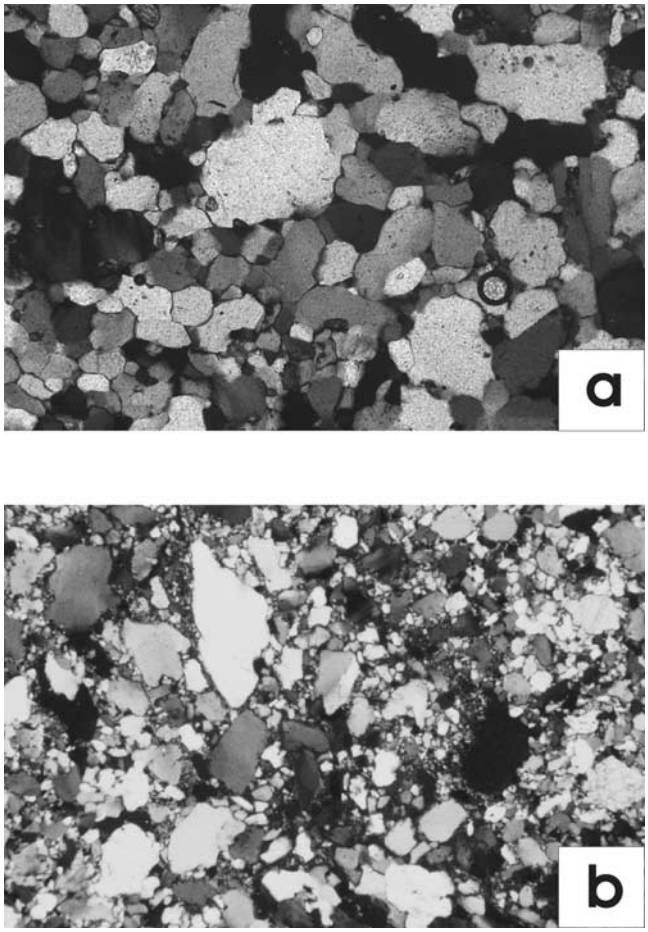

Figure 9. Thin sections under crossed polars of samples (a) NZ02-52 and (b) NZ02-61. The field of view is approximately 1.7 mm for Figure 9a and 3 mm for Figure 9b. The sarsen stone in Figure 9a is characterized by undulating, interlocking sutures between grains and very few impurities. It was extremely hard and has a minimum ^{10}Be age of 410 ka. By contrast, the quartzite in Figure 9b contains a significant amount of clay minerals, and other impurities and grain boundaries are typical detrital, unsutured contacts. This rock was considerably weaker and more porous than that in Figure 9a and was eroding by exfoliation along bedding planes (Figure 8a). It has a minimum ^{10}Be age of 128 ka.

check this aspect of the sampling, and avoided analyzing those that were suspect on these grounds.

8. Discussion and Conclusions

[23] The most important result of this study is that we can now tie together the cosmogenic isotope evidence with the geomorphology to produce a quantitative, coherent and consistent account of how the nose of South Rough Ridge has propagated northward in the late Quaternary. *Jackson et al.* [2002] could not explain the clustering of the cosmogenic dates obtained from the quartzite boulders on the crest of South Rough Ridge, and inferred that these could be related to episodic propagation of the ridge. The geometry and uplift of the abandoned river terraces shows unequivocally that the drainage evolution is related to ridge growth as well as regional base level change. The elevation changes and the ^{10}Be exposure ages show that the ridge uplifted by $\sim$60 m and propagated by $\sim$800 m over the last 550 kyr. It is interesting to note that when the terrace positions and ages on the ridge axis are plotted (Figure 2c) they form a more regular pattern than the apparently episodic ages, perhaps suggesting that ridge propagation was relatively steady after all. However, whether or not the ridge propagated continuously (i.e., by semiregular earthquakes), the corresponding response of the drainage was not continuous; it involved instead the switching of the Oliverburn stream to new courses in discrete (or relatively rapid) events, leaving behind a series of terraces. The average propagation rates (0.8–1.5 mm yr^{-1}) and uplift rates (0.08–0.12 mm yr^{-1}) only differ from those estimated earlier by *Jackson et al.* [2002] because of the use of a different production rate. When the two data sets are normalized to the same production rate, the propagation and uplift rates are in agreement. The ratio of $\sim$10 between the rate of propagation and the rate of uplift is that expected in simple fault growth models, and is also observed elsewhere (see *Jackson et al.* [2002] for a discussion). However, a significant enigma raised by these estimates is that the propagation rates are too small to generate the observed $\sim$20 km length of South Rough in the time of $\sim$2 Myr that is thought to be available from stratigraphic evidence [*Youngson et al.*, 1998], though the uplift rate can generate the observed relief (300–400 m) in that time. Detailed discussion of the issue of fault growth styles is beyond the scope of this paper, but there are several possibilities: (1) the stratigraphic evidence may not be secure, (2) propagation rates were much faster earlier in the Quaternary, and (3) naive models of incremental growth by progressive lengthening of single fault segments [e.g., *Jackson et al.*, 1996] are unrealistic. The apparent very rapid growth of large structures in a short time is not a situation peculiar to Central Otago: *Goldsworthy and Jackson* [2001] describe active faults in central Greece that must have initiated, grown to lengths of $\sim$20 km, and achieved offsets of at least 1–2 km, all in the space of 1–2 Myr. There too, late Quaternary fault slip rates can produce the total observed offset in the time available, but early propagation rates must have been very fast. Suggestion (3) is very probable, and it may be that the early growth of faults involves the rapid merger along strike of small fault segments that join up to achieve a substantial length quickly, before settling down to smaller propagation rates as offsets on the fault accumulate, in a manner simulated in the models of *Cowie* [1998].

[24] The demonstration of a coherent story between the geomorphology and relative cosmogenic ^{10}Be exposure ages requires that the quartzites on South Rough Ridge are not in steady state relative to erosion, in spite of apparent minimum exposure ages as great as 661 ka. This behavior is clearly a consequence of the extremely low erosion rates in the quartzites themselves, caused mostly by their hard, resistant nature and interlocking grain structure, and helped by the low annual rainfall of $\sim$300 mm yr^{-1}. With the much older ages of 750–1400 ka on the higher Rough Ridge, where erosion rates related to wind, rain and ice are likely to be higher, not lower, than on South Rough Ridge, there is the real possibility that even quartzites with

minimum ^{10}Be exposure ages significantly older than 600 ka may not be in saturated steady state with respect to erosion.

[25] In a regional context, the combination of isotopic data and detailed study of the geomorphology provides evidence that cosmogenic dating can be used to give valuable insights into the growth of the other ranges in Central Otago, and future papers will broaden this study to the other ranges. Of more general significance is that the extremely old ages and low erosion rates in this region allow us to study the evolution of anticlines over long time periods, and gain insights into the growth style and rates of these blind reverse faults.

[26] **Acknowledgments.** This work was supported by NERC grant NER/A/S/2001/00543 and the NERC Centre for Observation and Modeling of Earthquakes and Tectonics (COMET), the British-French Alliance program, the University of Otago Research Committee, and the Public Good Science Fund of New Zealand. Tandétron operation is supported by the CNRS (IN2P3, and INSUE). We thank Hélène Imbaud for invaluable help with the cosmogenic sample preparation. We thank NASA and the Jet Propulsion Lab AIRSAR group for providing the TOPSAR DEM. We would like to thank Rebecca Bendick, Paul Bierman, Mike Leeder, John Stone, and an anonymous reviewer for comments and communications that improved this paper. We also thank Mr. and Mrs. R. Gibson of Oliverburn station for allowing us frequent access to their land. This is Cambridge Earth Science contribution 8027.

References

Belton, D. X., R. W. Brown, B. P. Kohn, D. Fink, and K. A. Farley (2004), Quantitative resolution of the debate over antiquity of the central Australian landscape: Implications for tectonic and geomorphic stability of cratonic interiors, *Earth Planet. Sci. Lett.*, *219*, 21–34.

Bierman, P. R., and M. Caffee (2002), Cosmogenic exposure and erosion history of Australian bedrock landforms, *Geol. Soc. Am. Bull.*, *114*, 787–803.

Bierman, P. R., M. W. Caffee, P. T. Davis, K. Marsella, M. Pavich, P. Colgan, D. Mickelson, and J. Larsen (2002), Rates and timing of Earth surface processes from in situ-produced cosmogenic ^{10}Be, in *Beryllium: Mineralogy, Petrology, and Geochemistry*, *Rev. Mineral. Geochem.*, vol. 50, edited by E. S. Grew, pp. 147–205, Mineral. Soc. of Am., Washington, D. C.

Bishop, D. G. (1994), Extent and regional deformation of the Otago peneplain, *Sci. Rep. 94/1*, 10 pp., Inst. of Geol. and Nucl. Sci., Lower Hutt, New Zealand.

Brook, E. J., E. T. Brown, M. D. Kurz, R. P. Ackert, G. M. Raisbeck, and F. Yiou (1995), Constraints on age, erosion, and uplift of Neogene glacial deposits in the Transantarctic Mountains determined from in situ cosmogenic ^{10}Be and ^{26}Al, *Geology*, *23*, 1063–1066.

Brown, E. T., J. H. Edmond, G. M. Raisbeck, F. Yiou, M. D. Kurz, and E. J. Brook (1991), Examination of surface exposure ages of Antarctic moraines using in situ produced ^{10}Be and ^{26}Al, *Geochim. Cosmochim. Acta*, *55*, 2269–2283.

Cotton, C. A. (1917), Block mountains in New Zealand, *Am. J. Sci.*, *44*, 249–293.

Cowie, P. A. (1998), A healing-reloading feedback control on the growth rate of seismogenic faults, *J. Struct. Geol.*, *20*, 1075–1087.

Goldsworthy, M., and J. Jackson (2001), Migration of activity within normal fault systems: Examples from the Quaternary of mainland Greece, *J. Struct. Geol.*, *23*, 489–506.

Gosse, J. C., and F. M. Phillips (2001), Terrestrial in situ cosmogenic nuclides: Theory and application, *Quat. Sci. Rev.*, *20*, 1475–1560.

Hotchkis, M., D. Fink, C. Tuniz, and S. Vogt (2000), Accelerator mass spectrometry analyses of environmental radionucleides: Sensitivity, precision and standardization, *Appl. Radiat. Isotopes*, *53*, 31–37.

Jackson, J., R. Norris, and J. Youngson (1996), The structural evolution of fault and fold systems in Central Otago, New Zealand: Evidence revealed by drainage patterns, *J. Struct. Geol.*, *18*, 217–234.

Jackson, J., J.-F. Ritz, L. Siame, G. Raisbeck, F. Yiou, R. Norris, J. Youngson, and E. Bennett (2002), Fault growth and landscape development rates in Otago, New Zealand, using in situ cosmogenic ^{10}Be, *Earth Planet. Sci. Lett.*, *195*, 185–193.

Lal, D. (1991), Cosmic ray labelling of erosion surfaces: In situ nucleide production rates and erosion models, *Earth Planet. Sci. Lett.*, *104*, 424–439.

Licciardi, J. M. (2000), Alpine glacier and pluvial lake records of late Pleistocene climate variability in the western United States, Ph.D. dissertation, Oreg. State Univ., Corvallis.

Raisbeck, G. M., F. Yiou, D. L. Bourlés, J. Lestringuez, and D. Deboffe (1987), Measurements of ^{10}Be and ^{26}Al with a Tandétron AMS facility, *Nucl. Instrum. Methods Phys. Res.*, *29*, 22–26.

Raisbeck, G. M., F. Yiou, D. L. Bourlés, E. T. Brown, D. Deboffe, P. Jouhanneau, J. Lestringuez, and Z. Q. Zhou (1994), The AMS facility at Gif-sur-Yvette: Progress, perturbations and projects, *Nucl. Instrum. Methods Phys. Res.*, *92*, 43–46.

Stone, J. (2000), Air pressure and cosmogenic isotope production, *J. Geophys. Res.*, *105*, 23,753–23,759.

Vance, D., M. Bickle, C. A. Ivy-Ochs, and P. W. Kubik (2003), Erosion and exhumation in the Himalaya from cosmogenic isotope inventories of river sediments, *Earth Planet. Sci. Lett.*, *206*, 273–288.

Youngson, J. H., D. Craw, C. A. Landis, and K. R. Schmitt (1998), Redefinition and interpretation of late Miocene—Pleistocene terrestrial stratigraphy, Central Otago, New Zealand, *N. Z. J. Geol. Geophys.*, *41*, 51–68.

Youngson, J. H., E. R. Bennett, J. A. Jackson, R. J. Norris, G. M. Raisbeck, and F. Yiou (2005), 'Sarsen stones' at German Hill, Central Otago, New Zealand, and their potential for in situ cosmogenic isotope dating of landscape evolution, *J. Geol.*, in press.

E. R. Bennett and J. A. Jackson, University of Cambridge, Department of Earth Sciences, Bullard Laboratories, Madingley Road, Cambridge CB3 OEZ, UK. (bennett@esc.cam.ac.uk)

E. Fielding, Jet Propulsion Laboratory, 4800 Oak Grove Drive, Pasadena, CA 91109, USA.

R. J. Norris and J. H. Youngson, Department of Geology, University of Otago, P.O. Box 56, Dunedin, New Zealand.

G. M. Raisbeck and F. Yiou, Centre de Spectrométrie Nucléaire et de Spectrométrie de Masse, IN2P3-CNRS, Bâtiment 108, F-91405 Orsay, France.